Theoretical components of the VASIMR plasma propulsion concept

Alexey V. Arefiev and Boris N. Breizman

Institute for Fusion Studies, The University of Texas, Austin, Texas 78712

(Dated: January 18, 2004)

Abstract

The ongoing development of the Variable Specific Impulse Magnetoplasma Rocket (VASIMR) involves basic physics analysis of its three major components: helicon plasma source, ion cyclotron-resonance heating (ICRH) module, and magnetic nozzle. This paper presents an overview of recent theoretical efforts associated with the project. It includes: 1) a first-principle model for helicon plasma source, 2) a nonlinear theory for the deposition of rf-power at the ion cyclotron frequency into plasma flow, and 3) a discussion of the plasma detachment mechanism relevant to VASIMR.

I. INTRODUCTION

This work has been motivated by the Variable Specific Impulse Magnetoplasma Rocket (VASIMR) project [1, 2], one of the prospective plasma-based space propulsion systems [3]. The VASIMR concept originated in the early 1980's as an attempt to design a thruster suitable for human interplanetary missions.

A relevant spaceship must be *fast* and it should have reasonable *abort options* for crew safety. The travel time must be minimized in order to reduce the crew's exposure to radiation and weightlessness. These requirements can be met by using a propulsion system with a *continuous thrust*.

A conventional chemical rocket accelerates in a short burst in the beginning of the journey and then it follows a ballistic trajectory to the point of final destination. In contrast with this, a spacecraft with a continuous thrust would spend roughly half of the travel time accelerating and the other half slowing down. Such a spacecraft is not constrained to a ballistic trajectory, so that its trajectory can be optimized in order to decrease the travel time. It is essential that continuous thrust gives the option of aborting the mission and returning back from early in the cruise.

It is generally desirable to have a thruster with *low propellant consumption* in order to cut down on propellant weight and increase useful payload. A rocket ejecting propellant of mass m with exhaust velocity u gains momentum mu. Therefore, by increasing the exhaust velocity, a propulsion system can be made more propellant-efficient without sacrificing the momentum gain. In a chemical rocket, the exhaust velocity is related to the combustion temperature. This temperature is limited by the energy stored in the chemical bonds of the reactants, which does not exceed few electron volts. A significant increase in the exhaust velocity would require at least 10 eV per particle. At these energies ionization occurs, so that one has to consider *plasma as a propellant*.

The energy required to produce a single electron-ion pair considerably exceeds the ionization potential, because the ionization is unavoidably accompanied by excitation and line radiation. The energy of the ions in the exhaust should be significantly above the ionization potential, since only in this case the major part of the energy will go into ion acceleration rather than into plasma production. The most favorable energy range per particle for *plasma-based propulsion systems* is in a range of hundreds of electron volts.

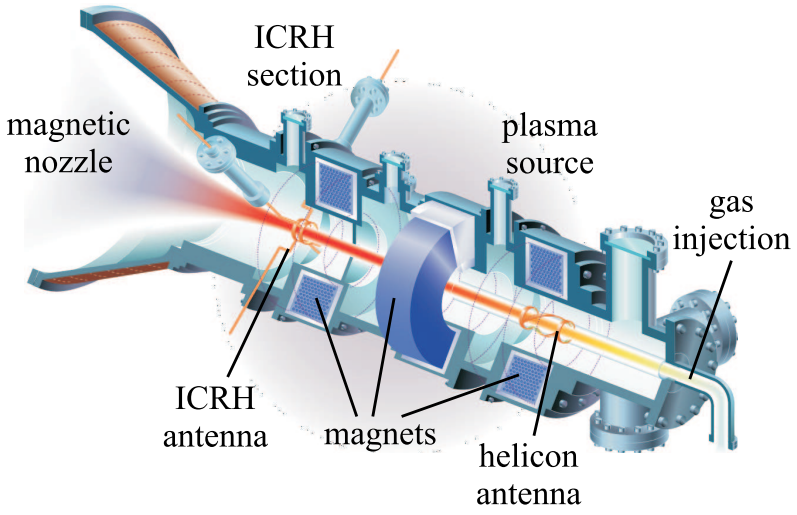

FIG. 1: The layout of VASIMR [1] (courtesy of NASA).

Plasma-based propulsion systems are not only capable of providing continuous thrust, but they also allow one to vary the exhaust velocity. A system with a variable velocity (variable specific impulse) can handle both the cruise phase of the journey and the maneuvering near the origin and destination planets. This characteristic makes plasma-based systems even more attractive.

It is important to point out that low propellant consumption of plasma-based systems is achieved through high energy consumption. An energy source that can release more than a hundred electron volts per fuel particle is needed. Otherwise, the mass of the energy source alone is going to be higher than the propellant mass. The only way to release this amount of energy is through a nuclear reaction. For this reason, a nuclear reactor would be a relevant energy source for plasma-based thrusters.

NASA is currently investigating several new plasma-based propulsion concepts offering high propellant efficiency. A distinctive feature of VASIMR is that it employs radio frequency electromagnetic waves to deliver power to the propellant. VASIMR does not require electrodes for plasma production or ion acceleration, so that the thruster lifetime is not limited by electrode erosion.

The schematic layout of VASIMR and its magnetic configuration are shown in Figs. 1 and 2 respectively. The device consists of three main components: the low energy plasma source, ion cyclotron-resonance heating (ICRH) section, and magnetic nozzle. The helicon source creates a cold plasma by ionizing the injected gas in a rf-discharge. A supersonic plasma

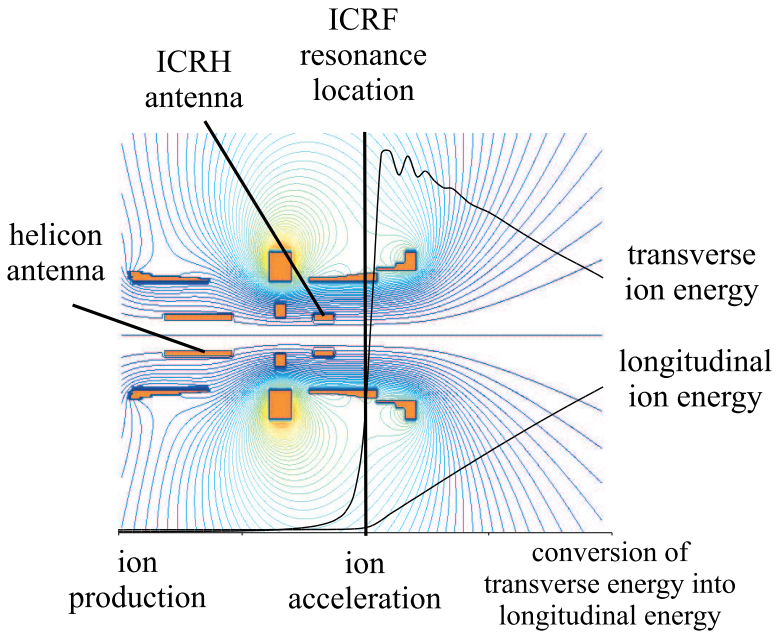

FIG. 2: Magnetic field configuration in VASIMR together with plots of ion energies. The ion energy plots demonstrate the ion-cyclotron resonant heating and the subsequent transformation of the gyro-motion into the axial motion along the magnetic field lines.

flow from the helicon source continues along the field lines, down the magnetic field gradient, into the ICRH section. The VASIMR concept employs ICRH as the main mechanism for rf-power deposition in the plasma. In the ICRH section, the ion gyro-frequency ω_{ci} matches the ICRH antenna frequency ω to ensure wave energy conversion into the ion gyro-motion. Following the magnetic field lines, the ions leave the ICRH section and enter the magnetic nozzle. The nozzle transforms the ion rotational motion into the axial motion (see Fig. 2) and ensures plasma detachment from the rocket.

The VASIMR concept is still at an early stage of its development. There is a wide range of engineering, experimental, and theoretical issues that are yet to be addressed. The focus of this paper is on the theoretical plasma physics aspects of the VASIMR concept. The paper deals with the basic physics of VASIMR with an attempt to single out problems of general interest that can also have applications beyond VASIMR. The specific problems solved in this work should be ultimately incorporated into an integrated model that describes all elements of VASIMR self-consistently.

The paper is organized in the following way: Sec. II presents a qualitative first-principle model of the helicon plasma source; Sec. III presents a first-principle theory for single-pass ion cyclotron heating; Sec. IV contains a qualitative discussion of the plasma detachment;

Sec. V is a summary.

II. HELICON PLASMA SOURCE OPERATION

Our study of the helicon plasma source has been motivated by the experiments aimed to develop a source suitable for VASIMR [2, 4]. The two distinctive features of the experiments are the use of light gases (H and He) for plasma production and plasma and gas flow through the source. Our goal is to achieve qualitative understanding of the source operation in order to optimize the source performance.

We describe the helicon plasma source by a self-consistent model that includes three major components, which are *rf-field structure*, *power balance*, and *particle balance*. Unlike recent semi-phenomenological model [5], our approach does not involve any free parameters or extra assumptions about plasma transport coefficients.

The source operation requires plasma eigenmode excitation for power deposition. Therefore, the *rf-field structure* is determined by the excited eigenmode. The operational rf-antenna frequency is such that the eigenmode stems from electron response without involvement of the ions.

The *rf-power* supplied by the antenna is absorbed by the electrons through the elastic electron-neutral and electron-ion collisions. The electrons lose their energy by exciting the background gas in inelastic collisions. This energy is being lost from the plasma via line radiation. The *power balance* is established locally by the electrons and it is insensitive to the ion dynamics.

The plasma is produced by fast electrons with energies above the ionization threshold. The plasma production does not affect the power balance, because the excitation rate is much faster than the ionization rate. The plasma production is balanced by the plasma transport that is determined by the ion mobility. The recombination rate is negligible compared to the ionization rate, because the degree of ionization is small. The *particle balance* problem is essentially a kinetic problem of ion transport under the effect of the ambipolar electric field and ion-neutral collisions.

The longest time-scale that characterizes the plasma source is the time required to establish a steady-state plasma density profile (τ_p), which is roughly the ion travel time through the source. For a given density profile, the power balance and steady-state rf-field structure

can be established on much shorter time scales than τ_p. The characteristic time of establishing a rf-field structure is roughly $1/\gamma$, where γ is the wave damping rate, whereas the characteristic time for the power balance is the energy confinement time (τ_E). The following ordering of the time scales is typical for the discharge:

$$\tau_p \gg \tau_E,\ 1/\gamma. \tag{1}$$

Guided by this ordering, we describe the evolution of the plasma density profile under assumption that the power balance and the rf-field structure establish instantaneously. Our self-consistent model consists of the following set of nonlinear equations:

$$\frac{\partial}{\partial r_\alpha}\frac{\partial E_\beta}{\partial r_\beta} - \frac{\partial^2 E_\alpha}{\partial r_\beta^2} - \frac{\omega^2}{c^2}\varepsilon_{\alpha\beta}E_\beta = \frac{4\pi i\omega}{c^2}j^a_\alpha, \tag{2}$$

$$\langle \mathbf{j}\cdot\mathbf{E}\rangle = P_{rad}, \tag{3}$$

$$\frac{\partial n}{\partial t} + \frac{1}{r}\frac{\partial}{\partial r}(r\psi_r) + \frac{\partial \psi_z}{\partial z} = nn_0\left\langle \sigma_{ion}v\right\rangle_e. \tag{4}$$

Equation (2) is the linear wave equation, where E_α is the electric field, j^a_α is the antenna current density, ω is the antenna operational frequency, and $\varepsilon_{\alpha\beta}$ the cold plasma dielectric tensor. Equation (3) is the local power balance condition, with the deposited rf-power on the left-hand side and the radiated power (P_{rad}) on the right-hand side. The rf-power deposition is a product of the plasma current $\mathbf{j}$ and the wave electric field $\mathbf{E}$, averaged over the wave period. We assume that the electron distribution is Maxwellian [17], because $\tau_E\nu_{ee} \gg 1$, where ν_{ee} is the electron-electron collision frequency. Therefore, P_{rad} should be expressed in terms of electron temperature T_e. Equation (4) is the continuity equation for the plasma density $n(\mathbf{r},t)$. It is obtained by velocity integration of the ion kinetic equation. Here ψ_r and ψ_z are the radial and axial ion flux densities, that must be self-consistently expressed in terms of $T_e(\mathbf{r})$ and $n(\mathbf{r},t)$ using the ion distribution function. The corresponding ion distribution function in the presence of an ambipolar electric field and ion-atom charge-exchange and elastic collisions has been calculated in Ref. [6]. The right-hand side of Eq. (4) describes the ionization of the background gas with density n_0 by electron impact at the rate $\left\langle \sigma_{ion}v\right\rangle_e$, calculated for the electron temperature T_e.

The key features of the discharge operation can be captured by a qualitative "zero-

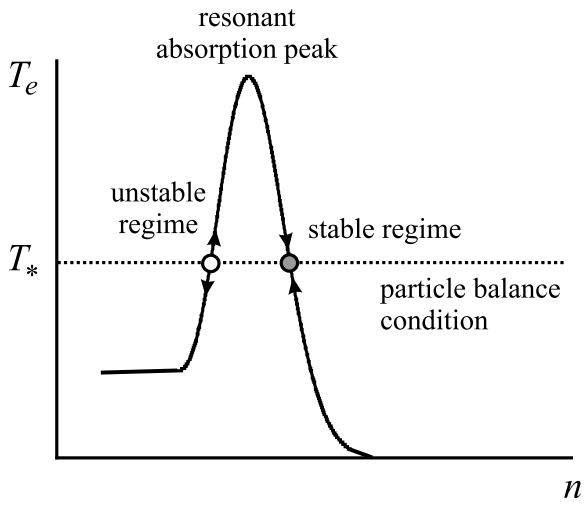

FIG. 3: Discharge stability diagram. Solid curve $T_e(n)$ represents possible states of the system. Dashed line represents the equilibrium temperature T_* determined from the particle balance condition. The intersection points are the system equilibria. The higher density equilibrium is stable (grey circle). The lower density equilibrium is unstable (white circle).

dimensional" picture, that assumes that the discharge at each moment is described by a characteristic plasma density n. For an instantaneous density profile, the electron temperature is uniquely determined from Eqs. (2) and (3). Then the possible states of the discharge in (T_e, n)-plane are represented by a corresponding curve $T_e(n)$ [7].

The curve $T_e(n)$ is not monotonic due to the eigenmode excitation as shown schematically in Fig. 3 by the solid curve. The rf-antenna excites the eigenmode only if the operational frequency is close to the eigenfrequency ω_*. This requires a specific value of the plasma density (n_*) determined by the dispersion relation. It is important that the dispersion relation involves the plasma density, but it does not involve the electron temperature, because the plasma is cold. For a fixed antenna current, the rf-power deposited by the antenna into the plasma sharply increases when n reaches n_*. The power balance condition establishes a one-to-one correspondence between T_e and the rf-power deposition, which readily gives a resonant-type temperature dependence $T_e(n)$.

It has been demonstrated in Ref. [6] that Eq. (4) is invariant with respect to a rescaling transformation $n \to \alpha n$, despite the fact that this equation is nonlinear. Hence, Eq. (4) determines just a functional dependence of n on $\mathbf{r}$ and t, but not the absolute value of the plasma density. In the steady-state regime, the plasma density significantly decreases towards the walls and towards the outlet of the source, so that the $n = 0$ boundary condition

can be assumed when solving Eq. (4). In order to satisfy this boundary condition, a specific value (T_*) of the *electron temperature* is required, given the gas content, the equilibrium magnetic field, and the dimensions of the source [6].

Intersections of the $T_e = T_*$ line and the solid curve in Fig. 3 represent the equilibrium states. While the value of T_* does not depend on the antenna current I_0, the rf-power deposition by the antenna is proportional to I_0^2, which means that the height of the $T_e(n)$-curve increases with I_0. Then there is a minimum value I_{cr} of the antenna current that is needed to sustain the discharge. For I_0 greater than I_{cr}, there are two points of intersection as shown in Fig. 3, i.e. two possible states of equilibrium. However, only the higher density equilibrium (dark circle in Fig. 3) is stable, while the lower density equilibrium is unstable (white circle in Fig. 3).

An important consequence of this picture is that the operational frequency always exceeds the eigenfrequency in the steady-state. The frequency shift is comparable to γ and thus it is very small. To lowest order, condition $\omega \approx \omega_*$ must be satisfied, which determines the characteristic plasma density in the discharge.

The plasma density is considerably nonuniform along the radius, which has a strong effect on the structure of the eigenmodes with *nonzero value* of the azimuthal mode number m [8–11]. The analysis of Eq. (2) performed in Ref. [9] shows that the relevant eigenmode is a helicon mode coupled to space charge effects from electron $\mathbf{E} \times \mathbf{B}$ drift. It has distinct features of a surface wave, as it is localized radially near the nonuniformity. VASIMR requires a sufficiently dense plasma with $\omega_{pe} a/c \gg 1$, where a is the characteristic radial scale of the density profile. In this regime, the dispersion relation is roughly given by [9]:

$$\omega \sim \omega_{ce} \frac{k_z^2 c^2}{\omega_{pe}^2}, \tag{5}$$

where k_z is the characteristic longitudinal wave number. Note that the applicability condition $\omega \gg \sqrt{|\omega_{ce}\omega_{ci}|}$ given in Ref. [9] is overly restrictive for the considered eigenmode. It can be shown that the dispersion relation (5) is also valid for $\omega \sim \sqrt{|\omega_{ce}\omega_{ci}|}$. Estimating k_z as π/L, where L is the length of the source, we find the following scaling for the plasma density:

$$n \sim \frac{\omega_{ce}}{\omega} \frac{m_e c^2}{e^2 L^2}. \tag{6}$$

This radially localized helicon mode has recently been identified experimentally [4].

The ion motion in the discharge is controlled by: ambipolar electric field resulting from quasineutrality; ion collisions with atoms; equilibrium magnetic field. The axial and radial ion transport are significantly different, because the ions are magnetized. The estimates of the total axial (Ψ_z) and radial (Ψ_r) ion fluxes are given by [6]:

$$\Psi_z \approx 2\pi a^2 \psi_z \approx \frac{n a^2 C_s}{\xi(\xi+1)} \frac{C_s}{a\omega_{ci}}, \tag{7}$$

$$\Psi_r \approx 2\pi a L \psi_r \approx \xi(\xi+1) n a^2 C_s \frac{C_s}{a\omega_{ci}}, \tag{8}$$

where

$$\xi \equiv \frac{C_s}{a\omega_{ci}} \sqrt{n_0 L \sigma_i}, \tag{9}$$

$C_s \equiv \sqrt{T_e/m_i}$ is the ion sound velocity, σ_i is the ion-atom collision cross-section, a and L are the characteristic radial and axial scales of the plasma density profile. The ratio between the fluxes is given by:

$$\frac{\Psi_r}{\Psi_z} = \xi^2(\xi+1)^2. \tag{10}$$

The longitudinal transport prevails when ξ is much smaller than unity, whereas the case $\xi \gg 1$ corresponds to predominantly radial transport.

The plasma flux out of the source must significantly exceed the flux to the walls in the regime relevant to VASIMR. This regime requires

$$R \gg \frac{C_s}{\omega_{ci}} \sqrt{n_0 L \sigma_i}, \tag{11}$$

where R is the radius of the source. Radial transport is negligible on the scale of R under condition (11). As a result, the characteristic radial scale of the density profile can be smaller than R. However, it can not be smaller than

$$a \approx \frac{C_s}{\omega_{ci}} \sqrt{n_0 L \sigma_i}, \tag{12}$$

because for the scale specified by Eq. (12) the radial transport across the plasma is comparable to the axial transport. It must be pointed out, that for the excited eigenmode with $m \neq 0$, the wave field amplitude is peaked off-axis and hence the ionization rate is peaked

off-axis as well. This indicates that the plasma density profile can be hollow under condition (11). It is noteworthy that, in the case of predominantly radial transport, an off-axis ionization cannot maintain a hollow plasma density profile [6].

The ion transport must balance ion production in steady-state regime. The particle balance condition for the case of predominantly axial plasma losses has the form: $nn_0 \langle \sigma_{ion} v \rangle_e L \approx \psi_z$. This readily gives the required value of the ionization rate:

$$\langle \sigma_{ion} v \rangle_e \approx \frac{C_s}{n_0 L \sqrt{n_0 L \sigma_i}}. \tag{13}$$

On the other hand, for a Maxwellian electron distribution with $T_e < \varepsilon_{ion}$ one can estimate $\langle \sigma_{ion} v \rangle_e$ as

$$\langle \sigma_{ion} v \rangle_e \approx 2\sqrt{\frac{2\pi T_e}{m_e}} \frac{e^4}{\varepsilon_{ion}^2} \exp\left[-\frac{\varepsilon_{ion}}{T_e}\right], \tag{14}$$

where ε_{ion} is the ionization threshold. Equations (13) and (14) determine the electron temperature required to sustain a steady-state discharge:

$$T_* \approx 2\varepsilon_{ion} \Big/ \ln\left[8\pi n_0^3 L^3 \frac{m_i}{m_e} \frac{\sigma_i e^8}{\varepsilon_{ion}^4}\right]. \tag{15}$$

It should be noted that T_* depends only on the gas content ($n_0 L$) and the dependence is relatively weak (logarithmic).

In order to estimate I_{cr}, we assume that ω matches the eigenfrequency. The collisional power dissipation in the radially localized helicon mode is associated with j_z. Thus the rf-power dissipation per unit volume can be estimated as $\langle j_z E_z \rangle \approx \nu_e E_z^2 \omega_{pe}^2 / \omega^2$, where E_z is the axial component of the wave electric field and ν_e is the frequency of the elastic electron-ion and electron-atom collisions. The resulting wave damping rate is roughly given by $\gamma \approx \nu_e \frac{c^2}{\omega_{pe}^2 a^2}$. Therefore, the mode remains weakly damped ($\gamma \ll \omega$) even for $\nu_e \sim \omega$, since $\frac{\omega_{pe}^2 a^2}{c^2} \gg 1$. For a hollow plasma density profile of thickness a and with radius comparable to the antenna radius R, the value of E_z can be estimated as [18]:

$$E_z \approx \frac{\omega}{\nu_e} \frac{\omega I_{cr}}{c^2}. \tag{16}$$

Then the rf-power dissipation is given by:

$$\langle j_z E_z \rangle \approx \frac{\omega_{pe}^2}{\nu_e} \frac{\omega^2 I_{cr}^2}{c^4}. \tag{17}$$

The power lost via gas excitation and subsequent line-radiation can be estimated as

$$P_{rad} \approx \sqrt{8\pi} \left(\frac{T_e}{m_e} \right)^{3/2} \frac{m_e n_0 n e^4}{T_e \varepsilon_{exc}} \exp\left[-\frac{\varepsilon_{exc}}{T_e} \right], \tag{18}$$

where ε_{exc} is the ionization threshold. The power balance condition (3) readily gives the estimate for the value of I_{cr} under the assumption that the electron-ion collisions are responsible for the rf-power absorption:

$$I_{cr} \approx c^2 \sqrt{\frac{m_e}{L}} \left(\frac{4\Lambda}{3} \frac{e^4 n_0 L}{T_* \varepsilon_{exc}} \frac{\omega_{ce}}{\omega} \right)^{1/2} \frac{c}{L\omega} \exp\left[-\frac{\varepsilon_{exc}}{T_*} \right], \tag{19}$$

where Λ is the Coulomb logarithm. It is appropriate to point out that the exponent is given by:

$$\exp\left[-\frac{\varepsilon_{exc}}{T_*} \right] \approx \left(8\pi n_0^3 L^3 \frac{m_i}{m_e} \frac{\sigma_i e^8}{\varepsilon_{ion}^4} \right)^{\varepsilon_{exc}/2\varepsilon_{ion}}, \tag{20}$$

so that I_{cr} is not exponentially sensitive to any of the parameters.

An important conclusion from the presented self-consistent model is that the plasma density in the steady-state regime is not sensitive to I_0. It follows from Eqs. (5) and (6) that the density can be increased either by decreasing the length of the source or by forcing the discharge to switch to an eigenmode with a larger axial wave number. Moreover, once the antenna current exceeds I_{cr}, the rf-power absorbed by the plasma is also relatively insensitive to I_0. Finally, we expect the electron temperature profile in the discharge to be nearly flat compared to the density profile due to exponential dependence of the ionization and excitation rates on T_e.

III. SINGLE-PASS ION CYCLOTRON RESONANCE ABSORPTION

The Ion Cyclotron Resonance Heating (ICRH) in VASIMR has two distinct features. First, each ion passes the resonance only once, gaining an energy that is much greater than the initial energy. Second, the ion motion is collisionless, i.e. the energy gain is limited not

by collisions but by the time the ion spends at the resonance while moving along the field lines. Therefore, the ion final energy, as well as the rf-power absorption efficiency, depend on the incident-flow velocity.

The key features of the single-pass ICRH can be captured by considering a flow of *cold ions* [19] in an equilibrium axisymmetric mirror magnetic field $\mathbf{B}_0$ in the presence of a circular polarized wave rotating in the "ion" direction that is launched nearly parallel to the magnetic field lines [12]. We choose z as the axis of symmetry assuming that B_{0z} is positive and that it decreases monotonically along z, with $B_{0z} \gg B_{0r}$. The problem is effectively one-dimensional, since one can neglect the dependence of the wave fields on the perpendicular coordinates. The basic set of nonlinear fluid-type equations for the electromagnetic field of the circular polarized wave and the steady-state supersonic ion flow has the following form [12]:

$$\frac{\partial E_+}{\partial z} = \frac{\omega B_+}{c}, \tag{21}$$

$$\frac{\partial B_+}{\partial z} = \frac{\omega_{pi}^2}{\omega_{ci} c} E_+ - \frac{4\pi i}{c} n e V_+, \tag{22}$$

$$V_z \frac{\partial V_+}{\partial z} = \frac{e}{m_i} E_+ + i(\omega - \omega_{ci}) V_+, \tag{23}$$

$$V_z \frac{\partial V_z}{\partial z} = -\frac{1}{8\pi m_i n} \frac{B_{0z}}{B_*} \frac{\partial |B_+|^2}{\partial z} - \frac{|V_+|^2}{2B_*} \frac{\partial B_{0z}}{\partial z}, \tag{24}$$

$$\frac{B_*}{B_{0z}} n V_z \equiv j = const. \tag{25}$$

The quantity E_+ is the amplitude of the circular wave electric field:

$$E_+(z) \equiv \frac{E_x + i E_y}{\sqrt{B_{0z}/B_*}} e^{i\omega t}, \tag{26}$$

where B_* is the value of the magnetic field at the point $\omega = \omega_{ci}$. The quantities B_+ and V_+ have similar definitions, with B_+ corresponding to the wave magnetic field and V_+ corresponding to the transverse component of the ion velocity. The quantities n and V_z are ion density and the parallel component of the ion velocity, which are time-independent.

Equations (21) and (22) are Maxwell's equations, which include full nonlinear ion current

and linearized electron current. The displacement current is neglected, assuming that $\omega_{pi} \gg \omega_{ci}$. Equation (23) is the transverse component of the ion momentum balance equation. Equation (24) is the axial momentum balance equation, with a convective term on the left-hand side and two axial forces on the right-hand side. The two forces in Eq. (24) are: 1) the ∇B-force, which is associated with the ion magnetic moment; 2) the time averaged Lorentz force from the wave. Equation (24) implies that the ions complete many cycles over their gyro-orbit while they move through the resonance. Equation (25) is the ion flux conservation law.

The boundary conditions for this set of equations are

$$V_+(-\infty) = 0 \tag{27}$$

(absence of the ion gyro motion at $z = -\infty$) and

$$E_+(+\infty) = 0, \qquad B_+(+\infty) = 0 \tag{28}$$

(evanescent wave fields downstream). In addition we specify the power flux in the incident wave, the incident ion flux, and the ion flow velocity at $z \to -\infty$. It should be noted that the incoming ion flow must be supersonic to justify this formulation of the problem. The quantities to be determined from Eqs. (21)-(25) are the ion energy gain and the reflection coefficient for the wave.

The regime of the power absorption depends on the incident power flux and incident flow velocity, as shown in Fig. 4 on the map of absorption regimes in the (γ, P) plane. The parameter γ is proportional to the incident flow velocity:

$$\gamma \equiv \frac{V_z}{l\omega}\left(\frac{l\omega_{pi}}{c}\right)^4, \tag{29}$$

whereas P is the incident power flux that we normalize by

$$P_* \equiv m_i n c^3 \left(\frac{l\omega}{c}\right)^3 \left(\frac{c}{l\omega_{pi}}\right)^{10}. \tag{30}$$

Here l is the characteristic-scale length of the equilibrium magnetic field near the resonance.

If the flow is sufficiently fast, then its velocity does not change significantly at the reso-

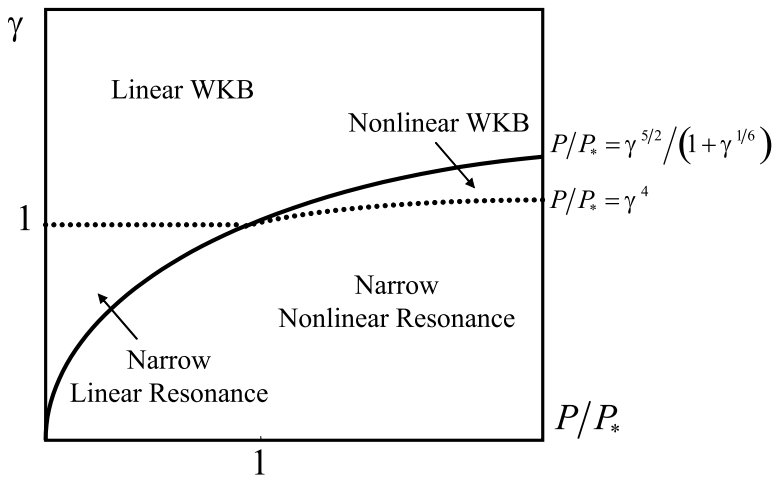

FIG. 4: Map of absorption regimes in the (γ, P) plane. Solid curve marks the border between linear and nonlinear regimes. Dashed curve shows the applicability boundary for WKB-description. The Narrow Nonlinear Resonance area corresponds to significant reflection of the incident wave.

nance. As a result, the ion density is also nearly constant throughout the resonance. In this regime, ion flux through the resonance turns out to be sufficient to absorb all the rf-power. Technically, the description of the fast flow case is a linear problem. The linear regime lays above the solid curve in Fig. 4. In contrast with the fast incoming flow, the slow flow case is essentially nonlinear (area below the solid curve in Fig. 4). Slow ions can be significantly accelerated along the magnetic field even before they reach their full rotational energy. The driving forces responsible for their acceleration are the ∇B-force and rf-pressure.

The energy flux transformation takes place in the area where the wave group-velocity is comparable to the ion flow velocity. Depending on plasma parameters and incident rf-power, the width of the transformation layer can either extend over many wavelengths (WKB regime) or be as short as a fraction of wavelength (Narrow Resonance regime).

Equations (21) - (25) describe both the resonant conversion of the incident wave energy into the ion rotational energy and the subsequent transformation of the ion rotation into their fast motion along the decreasing magnetic field. They present a self-consistent nonlinear model for the deposition of rf-power in the ion cyclotron frequency range into a steady state plasma flow. This model can be viewed as a nonlinear version of the magnetic beach problem [13] for ion-cyclotron waves. We found that the absorption coefficient for the wave is 100% as long as either linear theory or WKB approximation applies to the problem. Acceleration of the incoming ions due to the energy deposition from the wave adds nonlinear features to the absorption process. The longitudinal forces create a density gradient in the

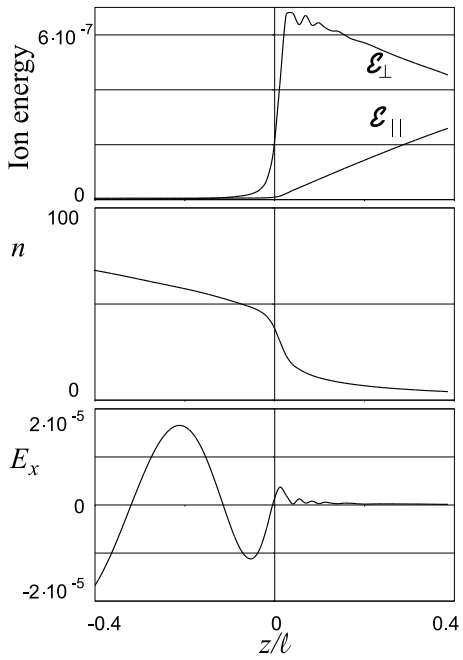

FIG. 5: Solution of Eqs. (21) - (25) for $j = 5 \cdot 10^5 (m_i \omega c^2)/(4\pi l e^2)$, $\bar{n} = 10^2 \cdot m_i c^2/4\pi e^2 l^2$, and $|\bar{E}| = \sqrt{10} \cdot 10^{-5} \cdot m_i l \omega^2/e$. The quantities $\mathcal{E}_\perp \equiv m_i |V_+|^2 B_{0z}/2B_*$ and $\mathcal{E}_\parallel \equiv m_i V_z^2/2$ are normalized to $m_i l^2 \omega^2$. The ion density n and the electric field component E_x are normalized to $m_i c^2/4\pi e^2 l^2$ and $m_i l \omega^2/e$ respectively.

ion flow, which causes partial reflection of the incident rf-power. The reflection is most pronounced when the characteristic scale-length of the density drop becomes shorter than the wavelength.

It should be mentioned, that the predicted density drop has been observed in recent single-pass ICRH experiments that demonstrate ion heating [14].

In order to illustrate the described features of single-pass ICRH, we have solved equations (21) - (25) numerically for the near-axis field of an open-ended solenoid:

$$B_{0z} = B_* \left[1 - \frac{z}{\sqrt{l^2 + z^2}} \right]. \tag{31}$$

Each solution is characterized by three parameters: the particle flux j, the mean density $\bar{n}$ and the mean electric field amplitude $|\bar{E}|$ in the incident flow ($z \to -\infty$).

Figure 5 shows a solution that represents a moderately nonlinear regime. The density plot in Fig. 5 already exhibits a steep gradient near the resonance, but with a minor reflection. The amount of reflection can be inferred from the oscillations of $|E|^2 \equiv E_x^2 + E_y^2$. These oscillations represent an interference between the incident and the reflected waves. Related

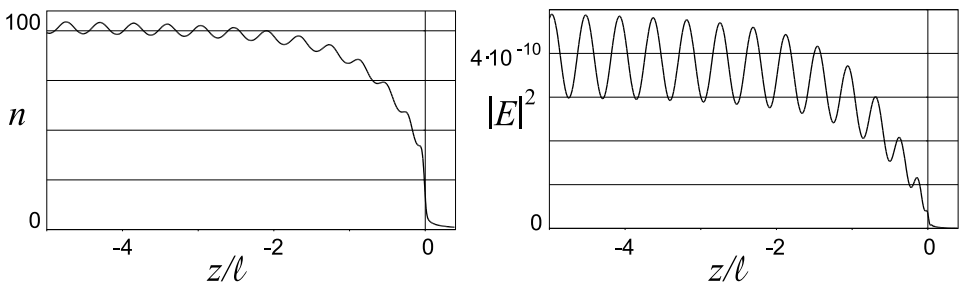

FIG. 6: Modulation of the ion density and wave amplitude due to nonlinear reflection from the resonance. The plots correspond to the solution with $j = 1.5 \cdot 10^5 (m_i \omega c^2)/(4\pi l e^2)$, $\bar{n} = 10^2 \cdot m_i c^2/4\pi e^2 l^2$, and $|\bar{E}| = 2 \cdot 10^{-5} \cdot m_i l \omega^2/e$. Quantities n and $|E|^2$ are normalized to $m_i l^2 \omega^2$ and $m_i^2 l^2 \omega^4/e^2$ respectively.

to the reflection are velocity and density modulations in the incoming flow (see Fig. 6).

Simple one-dimensional fluid-type model and simulations, presented in this section allow us to quantitatively model the entire process of wave energy conversion into the directed energy of the ion flow. For practical applications, the basic nonlinear effects discussed in this section need to be combined with two-dimensional calculations of the wave field. The need for such an extension becomes evident if one takes into account that the finite plasma radius should definitely affect the field structure in a realistic geometry.

The presented absorption model assumes that there is a wave propagating nearly parallel to the magnetic field lines towards the resonance. However, launching the relevant wave into the plasma is an important issue itself. In order to estimate the power that can be deposited into the $m = -1$ harmonic (a circular polarized wave rotating in the "ion" direction), one can consider a uniform plasma cylinder with radius r_p in a uniform equilibrium magnetic field B_0. It is important to emphasize that $r_p \ll c/\omega_{pi}$ for the parameters relevant to the VASIMR. Then a dual half-turn antenna [14] with radius r_a, length l_a, and current I_a deposits the following power into the $m = -1$ harmonic:

$$Q = \frac{\omega |k_0 l_a| l_a}{\pi^2 c^2} \frac{r_p^2}{r_a^2} I_a^2, \tag{32}$$

where

$$k_0 \equiv \frac{\omega}{c} \sqrt{\frac{\varepsilon + g}{2}}. \tag{33}$$

Quantities ε and g are the components of the cold plasma dielectric tensor:

$$\varepsilon + g = 1 - \sum_{\alpha} \frac{\omega_{p\alpha}^2}{(\omega - \omega_{c\alpha})\omega}, \tag{34}$$

were the subscript α labels particle species (electrons and ions).

It follows from Eq. (32) that the deposited power can be maximized by positioning the antenna close to the plasma, so that $r_a \approx r_p$. The maximum power is proportional to the square of the antenna length, but it is independent of the radius.

Note that Eq. (32) can also be written as $Q = Z_p I_a^2$, where Z_p is the corresponding plasma impedance. In order to efficiently deposit power into the plasma, the experimental parameters must be chosen such that Z_p exceeds the impedance of the rf-circuit.

Finally, Eq. (32) allows us to estimate the upper limit on the ion energy gain, which is Q divided by the total ion flux. This value can be maximized by increasing I_a for a given antenna.

IV. MAGNETIC NOZZLE AND PLASMA DETACHMENT CONCEPT

The role of the magnetic nozzle in VASIMR is to shape the outgoing plasma flow that creates thrust to propel the rocket. The thrust is produced by the ions pushing against the vacuum magnetic field on their way out of the nozzle. The plasma flow detaches from the thruster when its energy density exceeds the energy density of the guiding magnetic field. At this point the magnetic field is no longer strong enough to control the flow.

There are two stages in generating the thrust: accelerating the incoming plasma flow and detaching the flow from the rocket. At the entrance to the magnetic nozzle, the energy of the ion gyro-motion ($K_\perp = m_i v_\perp^2/2$) significantly exceeds the energy of the axial motion $\left(K_\parallel = m_i v_\parallel^2/2\right)$. The acceleration of the flow takes place in a strong magnetic field, which is not affected by the plasma. The magnetic field in the nozzle decreases gradually along the diverging field lines. Since the ion magnetic moment $\mu = m_i v_\perp^2/2B$ and total ion kinetic energy $K_i = K_\parallel + K_\perp$ are conserved, the nozzle transforms the ion rotational motion into the axial motion, accelerating the plasma flow. The axial velocity $v_\parallel$ becomes constant downstream, where the magnetic field is significantly smaller than that at the entrance.

The detachment of the plasma flow from the vacuum field lines can occur after the

energy density of the magnetic field ($B^2/8\pi$) drops below the kinetic energy density of the plasma flow ($n_i K_\parallel$) [15]. The latter can be achieved in a nozzle with straight diverging field lines. Indeed, it follows from the conservation of the magnetic flux that the magnetic field scales as $1/S$, where S is the nozzle cross section. Ion flux conservation requires that $n_i v_\parallel S$ stays constant. Also, $v_\parallel$ is constant when the ion energy is mostly in the parallel motion. Therefore, the kinetic energy density of the plasma flow ($n_i K_\parallel$) decreases as $1/S$, while the energy density of the magnetic field ($B^2/8\pi$) decreases as $1/S^2$ and thus eventually becomes smaller than $n_i K_\parallel$.

It is noteworthy, that the transition from a region with a strong magnetic field $\left(B^2/8\pi \gg n_i K_\parallel\right)$ to a region with a weak magnetic field $\left(B^2/8\pi \ll n_i K_\parallel\right)$ corresponds to a transition from a sub-Alfvénic ($v_\parallel \ll V_A$) to a super-Alfvénic flow ($v_\parallel \gg V_A$). All the magnetic field perturbations in the super-Alfvénic flow propagate only downstream. In this sense, the magnetic nozzle is analogous to a conventional Laval nozzle, which transforms a subsonic flow into a supersonic flow.

The plasma flow continues along the straight vacuum magnetic field lines after the transition and comes out of the magnetic nozzle highly super-Alfvénic. It then stretches the magnetic field lines and keeps moving away from the rocket conserving its axial momentum. The total axial momentum flux in this flow represents the thrust, that can be estimated as $\Phi\sqrt{2m_i K_i}$. Here Φ and K_i are the total ion flux and the ion kinetic energy in the incoming flow provided by the ICRH section. Note that K_i is roughly the ion energy gain due to the cyclotron heating.

The MHD description of the outgoing plasma flow relies on the frozen-in condition. The electrons follow the field lines closer than the ions, which may cause some charge separation due to large ion Larmor radius. However, this charge separation cannot be significant as long as the characteristic scale-length is much larger than the Debye length, which is an easy to satisfy requirement. The electrons are tied to the field lines due to their small Larmor radius and they are also tied to the ions due to the small Debye length. That way, the frozen-in condition is relevant even at large ion Larmor radii. It should also be pointed out that the curvature of the magnetic field lines is no longer controlled by the external coils once the plasma flow in the magnetic nozzle becomes super-Alfvénic. Instead, the plasma flow itself stretches the field lines. There is a good reason to believe that low-frequency MHD instabilities in the outgoing plasma flow are not nearly as dangerous as they are in magnetic

confinement devices simply because the ion life-time in VASIMR is extremely short. A more subtle question, so far open, is about higher frequency instabilities that could potentially break the frozen-in condition due to anomalous resistivity.

Finally, note that there is a direct similarity between the super-Alfvénic plasma detachment and the solar-wind formation. In a similar fashion, streaming outward from the sun plasma stretches the solar magnetic field forming the solar-wind [16].

V. SUMMARY

In this work, we have considered the main building blocks of the VASIMR concept: the helicon plasma source, the ion cyclotron-resonance heating (ICRH) section, and the magnetic nozzle. The theoretical plasma physics aspects of helicon plasma sources and ICRH have been analyzed with a focus on issues of general interest that are not limited to VASIMR. The specific problems solved in this work should be ultimately incorporated into an integrated model that describes all elements of VASIMR self-consistently. This is an ongoing investigation that may still reveal some new essential elements. So far, the key results of our research can be summarized as follows:

• New (radially localized) helicon modes in nonuniform plasma have been found. Similarly to electromagnetic waves in coaxial wave guide, these modes are characterized by unusually low frequency. These modes are likely to be responsible for the high efficiency of helicon sources at low frequencies.

• A first-principle theory for helicon discharge has been developed with a self-consistent treatment of the particle balance, power balance, and rf-field structure.

• A first-principle theory has been developed for single-pass ion cyclotron resonance absorption in the presence of a directed ion flow through the resonance. This problem presents a nonlinear generalization of the classical magnetic beach problem.

• High beta detachment concept is shown to be applicable to VASIMR.

Acknowledgments

This work was supported by the VASIMR Plasma Thruster project at NASA and by the U.S.Department of Energy Contract No. DE-FG03-96ER-54346. We thank Dr. Franklin

Chang-Dìaz, Dr. Roger Bengtson, and Dr. Martin Panevsky for stimulating discussions. We also thank Dr. Jarred Squire for providing us with experimental data from the VX-10 facility.

---

[1] F.R.Chang-Dìaz, Sci. Am. **283**, 90 (2000).

[2] F.R.Chang-Dìaz, J.P.Squire, A.V.Ilin, *et al.*, in *Proceedings of the International Conference on Electromagnetics in Advanced Applications (ICEAA 99), Torino, Italy* (Litografia Geda, Torino, 1999), p. 99.

[3] M.Martinez-Sanchez and J.E.Pollard, Journal of Propulsion and Power **14**, 688 (1998).

[4] M.Panevsky and R.Bengtson, "Characterization of the resonant electromagnetic mode in helicon discharges", submitted to Phys. Plasmas.

[5] M.D.Carter, F.W.Baity, G.C.Barber, R.H.Goulding, Y.Mori, D.O.Sparks, K.F.White, E.F.Jaeger, F.R.Chang-Dìaz, and J.P.Squire, Phys. Plasmas **9**, 5097 (2002).

[6] B.N.Breizman and A.V.Arefiev, Phys. Plasmas **9**, 1015 (2002).

[7] K.P.Shamrai, Plasma Sources Sci. Technol. **7**, 499 (1998).

[8] A.V.Gordeev and L.I.Rudakov, Sov. Phys. JETP **28**, 1226 (1968).

[9] B.N.Breizman and A.V.Arefiev, Phys. Rev. Lett. **84**, 3863 (2000).

[10] I.D.Sudit and F.F.Chen, Plasma Sources Sci. Technol. **3**, 602 (1994).

[11] A.V.Arefiev, Ph.D. thesis, University of Texas at Austin (2002).

[12] B.N.Breizman and A.V.Arefiev, Phys. Plasmas **3**, 907 (2001).

[13] T.H.Stix, *Waves in Plasmas* (AIP, New York, 1992), p.342.

[14] F.R.Chang-Dìaz, J.P.Squire, A.V.Ilin, *et al.*, Bull. Am. Phys. Soc. **48** (2003).

[15] E.B.Hooper, Journal of Propulsion and Power **9**, 757 (1993).

[16] E.N.Parker, Ap.J. **128**, 664 (1958).

[17] One can expect the electron distribution to differ from the Maxwellian when the axial rf electric field E_z is sufficiently strong to make the electron oscillatory energy comparable to the electron temperature T_e ($T_e \lesssim e^2E_z^2/m_e\omega^2$). We assume lower fields in our model ($T_e \gg e^2E_z^2/m_e\omega^2$), so that the assumption about the Maxwellian distribution is internally consistent. It is also relevant to the present VASIMR parameters.

[18] We assume that the electron oscillatory energy is smaller than T_e ($e^2E_z^2/m_e\omega^2 \ll T_e$), so that

the electron collision rate is determined by the electron temperature and it does not depend on the wave amplitude.

[19] The incoming flow is assumed to be supersonic, so that the ion velocity spread is negligible and the ions can be considered to as cold.